Sub-leading flow modes in PbPb collisions at $\sqrt{s_{\rm NN}} = 2.76$ TeV from the HYDJET++ model*

P. Cirkovic[1] D. Devetak[2] M. Dordevic[2] J. Milosevic[2,3;1)] M. Stojanovic[2]

[1] University of Belgrade and Institute of physics, P.O. Box 68, 11081 Belgrade, Serbia
[2] University of Belgrade and Vinča Institute of Nuclear Sciences, P.O. Box 522, 11001 Belgrade, Serbia
[3] University of Oslo, Department of Physics, Oslo, Norway

Abstract: Recent LHC results on the appearance of sub-leading flow modes in PbPb collisions at 2.76 TeV, related to initial-state fluctuations, are analyzed and interpreted within the HYDJET++ model. Using the newly introduced Principal Component Analysis (PCA) method applied to two-particle azimuthal correlations extracted from the model calculations, the leading and sub-leading flow modes are studied as a function of the transverse momentum ($p_{\rm T}$) over a wide centrality range. The leading modes of the elliptic ($v_2^{(1)}$) and triangular ($v_3^{(1)}$) flow calculated with the HYDJET++ model reproduce rather well the $v_2\{2\}$ and $v_3\{2\}$ coefficients measured experimentally using the two-particle correlations. Within the $p_{\rm T} \leqslant 3$ GeV/c range, where hydrodynamics dominates, the sub-leading flow effects are greatest at the highest $p_{\rm T}$ of around 3 GeV/c. The sub-leading elliptic flow mode ($v_2^{(2)}$), which corresponds to the $n=2$ harmonic, has a small non-zero value and slowly increases from central to peripheral collisions, while the sub-leading triangular flow mode ($v_3^{(2)}$), which corresponds to the $n=3$ harmonic, is even smaller and does not depend on centrality. For $n=2$, the relative magnitude of the effect measured with respect to the leading flow mode shows a shallow minimum for semi-central collisions and increases for very central and for peripheral collisions. For the $n=3$ case, there is no centrality dependence. The sub-leading flow mode results obtained from the HYDJET++ model are in rather good agreement with the experimental measurements of the CMS Collaboration.

Keywords: hydrodynamics flow, initial-state fluctuations, principal component analysis, HYDJET++

PACS: 25.75.Gz, 25.75.Dw **DOI:** 10.1088/1674-1137/41/7/074001

1 Introduction

According to Quantum Chromodynamics, at sufficiently high energy density, which can be achieved in ultra-relativistic heavy-ion collisions, a new state of matter, called Quark-Gluon Plasma (QGP), is created. One of the main features of the QGP is its collective expansion, which can be described by relativistic hydrodynamic flows. Due to the different pressure gradients in different directions, the initial spatial eccentricity converts into momentum anisotropy, observed in the final state as a preferential emission of particles in a certain plane.

Quantitatively, the anisotropic hydrodynamic flow is described by Fourier decomposition of the hadron yield distribution over azimuthal angle, ϕ, [1–3]

$$\frac{{\rm d}N}{{\rm d}\phi} \propto 1+2\sum_n v_n \cos[n(\phi-\Psi_n)], \qquad (1)$$

where the Fourier coefficients, v_n, characterize the magnitude of the azimuthal anisotropy measured with respect to the flow symmetry plane angle, Ψ_n. The angle Ψ_n determines the direction of maximum final-state particle density and can be reconstructed from the emitted particles themselves. The most analyzed anisotropic flow is the second order Fourier coefficient, v_2, called the elliptic flow. The angle Ψ_2 corresponds to the flow symmetry plane, which is correlated with the participant plane spanned over the beam direction and the shorter axis of the approximately elliptical shape of the nucleon overlap region. Due to the initial-state fluctuations of the position of nucleons at the moment of impact, higher-order deformations of the initial geometry are induced, which lead to the appearance of higher-order Fourier harmonics (v_n, $n \geqslant 3$ in Eq. (1)). They are measured with respect to the corresponding flow symmetry plane angles, Ψ_n [4]. The collective behavior of a strongly-coupled hot and dense QGP has been studied using the azimuthal anisotropy of emitted particles detected at experiments at the Relativistic Heavy Ion Collider (RHIC) [5–7]. The

Received 13 February 2017, Revised 22 March 2017

∗ Supported by Ministry of Education, Science and Technological Development of the Republic of Serbia (171019)

1) E-mail: Jovan.Milosevic@cern.ch

studies have been continued also with the experiments [8–19] at the Large Hadron Collider (LHC), where significantly higher collision energies are achieved.

Another experimental method to determined the v_n coefficients uses two-particle azimuthal correlations [20]. These correlations can be also Fourier decomposed as

$$\frac{\mathrm{d}N^{\mathrm{pair}}}{\mathrm{d}\Delta\phi}\propto 1+2\sum_n V_{n\Delta}\cos(n\Delta\phi), \tag{2}$$

where $\Delta\phi$ is the relative azimuthal angle of a particle pair. The two-particle Fourier coefficient $V_{n\Delta}$ is expected to factorize as

$$V_{n\Delta}(p_{\mathrm{T}}^a,p_{\mathrm{T}}^b)=v_n(p_{\mathrm{T}}^a)v_n(p_{\mathrm{T}}^b), \tag{3}$$

into a product of the anisotropy harmonics v_n.

A key assumption for the correctness of Eq. (3) is that the flow symmetry plane angle Ψ_n in Eq. (1) is a global quantity for a given collision. The effect has been theoretically predicted in Refs. [21, 22]. It is shown that even if the hydrodynamic flow is the only source of the two-particle correlations, initial-state fluctuations turn the flow symmetry plane from a global quantity to one dependent on both p_{T} and η. Lumpy hot-spots raised from the initial-state fluctuations can generate a local pressure gradient which makes the corresponding local flow symmetry plane slightly different but still correlated with the global flow symmetry plane. This effect of initial-state fluctuations thus breaks the factorization relation of Eq. (3). A significant breakdown of the factorization assumption expressed through Eq. (3) has been observed in both the transverse p_{T} and longitudinal η direction[1)] in symmetric PbPb collisions [18, 19, 23] as well as in asymmetric pPb collisions [19, 23].

Recently, a new approach has been introduced which employs Principal Component Analysis (PCA) to study the flow phenomena [24, 25]. Using a PCA approach, $V_{n\Delta}$ coefficients of the observed two-particle azimuthal correlations as a function of both particles p_{T} are represented through the leading and the sub-leading flow mode terms. The leading flow modes are essentially equivalent to anisotropy harmonics ($v_n\{2\}$) extracted from two-particle correlation methods. As a consequence of initial-state fluctuations, the sub-leading flow modes could appear as the largest sources of factorization breaking. The PCA study of this effect can give new insights into the expansion dynamics of strongly coupled QGP, and serves as an excellent tool for testing the hydrodynamical models.

This paper is organized in the following way. The basic features of the HYDJET++ model [26] are described in Section 2. Details of the applied construction of the two-particle correlation functions, as well as the PCA approach in flow analysis are given in Section 3. Using the HYDJET++ model, approximately 40M PbPb collisions at $\sqrt{s_{NN}}$=2.76 TeV are simulated and analyzed. The obtained results, together with the corresponding discussion, are given in Section 4. The results are presented over a wide range of centralities going from ultra central (0–0.2% centrality[2)]) up to peripheral (50%–60% centrality) PbPb collisions. The analyzed p_{T} interval is restricted to the $p_{\mathrm{T}}\leqslant 3$ GeV/c range where hydrodynamics dominates. A disscussion concerning the results obtained under different HYDJET++ model switches is given in Section 5. Conclusions are given in Section 6.

2 HYDJET++

The Monte Carlo HYDJET++ model simulates relativistic heavy ion collisions in an event-by-event manner. It is made of two components which simulate soft and hard processes. The soft part provides the hydrodynamical evolution of the system while the hard part describes multiparton fragmentation within the formed medium. Within the hard part, jet quenching effects are also taken into account. The minimal transverse momentum $p_{\mathrm{T}}^{\mathrm{min}}$ of hard scattering of an incoming parton regulates whether it contributes to the soft or to the hard part. Partons which are produced with $p_{\mathrm{T}}<p_{\mathrm{T}}^{\mathrm{min}}$, or which are quenched below $p_{\mathrm{T}}^{\mathrm{min}}$, do not contribute to the hard part. The hard part of the model consists of PYTHIA [27] and PYQUEN [28] event generators. These generators simulate initial parton-parton collisions, radiative energy loss of partons and parton hadronization. Within the soft part of the HYDJET++ model, the magnitude of the elliptic flow is regulated by spatial anisotropy $\epsilon(b)$, which is the elliptic modulation of the final freeze-out hypersurface at a given impact parameter vector[3)] magnitude b, and by momentum anisotropy $\delta(b)$, which gives the modulation of the flow velocity profile. The additionally introduced triangular modulation of the freeze-out hyper-surface, ϵ_3, determines the v_3 magnitude. The events can be generated under several switches. The most realistic one, 'flow+quenched jets', includes both hydrodynamics expansion and quenched jets. In this analysis, the pure 'flow' switch is also used. The details of the model can be found in the HYDJET++ manual [26].

1) Pseudorapidity η is defined as $-\ln\tan(\theta/2)$ where θ is the polar angle.

2) The centrality in heavy ion collisions is defined as a fraction of the total inelastic PbPb cross section, with 0 denoting the most central collisions.

3) In an ideal circle-like geometry, impact parameter $\vec{b}$ is a vector which connects the centers of the colliding nuclei.

3 Prescription of the principal component analysis technique

3.1 Two-particle correlation function

The construction of the two-dimensional two-particle correlation function follows the definition adopted within the CMS experiment. Any charged pion from the $|\eta|<2$ range can be used as a 'trigger' particle. In order to perform a differential analysis, all events are divided into eight centrality classes, while the analyzed $p_{\rm T}$ range has seven non-equidistant intervals. Since in an event there can be more than one trigger particle from a given $p_{\rm T}$ interval, the corresponding total number is denoted by $N_{\rm trig}$. In each event, every trigger particle is paired with all of the remaining charged pions from the $|\eta|<2$ range within a given $p_{\rm T}$ interval. The signal distribution, $S(\Delta\eta,\Delta\phi)$, is defined as the yield of the per-trigger-particle pairs within the same event,

$$S(\Delta\eta,\Delta\phi)=\frac{1}{N_{\rm trig}}\frac{{\rm d}^2N^{\rm same}}{{\rm d}\Delta\eta{\rm d}\Delta\phi}. \tag{4}$$

In Eq. (4), $N^{\rm same}$ denotes the per-trigger-particle pairs yield within a given $(\Delta\eta,\Delta\phi)$ bin where $\Delta\eta$ and $\Delta\phi$ are corresponding differences in pseudorapidity and azimuthal angle between the two charged pions which are forming the pair. The background distribution, denoted with $B(\Delta\eta,\Delta\phi)$, is constructed using the technique of mixing topologically similar events which ensure that the pairs are not physically correlated. Here, topological similarity means that events which are mixed have relative difference in multiplicity smaller than 5%. The trigger particles from one event are combined (mixed) with all of the associated particles from a different event. In order to reduce the contribution to the statistical uncertainty from the background distribution, associated particles from 10 randomly chosen events are used. In the background distribution, defined as

$$B(\Delta\eta,\Delta\phi)=\frac{1}{N_{\rm trig}}\frac{{\rm d}^2N^{\rm mix}}{{\rm d}\Delta\eta{\rm d}\Delta\phi}, \tag{5}$$

$N^{\rm mix}$ denotes the number of mixed-event pairs in a given $(\Delta\eta,\Delta\phi)$ bin. Due to the fact that pairs are formed from uncorrelated particles, the background gives a distribution of independent particle emission.

The two-dimensional two-particle differential correlation function is then defined as the normalized ratio of the signal to the background distribution

$$\frac{1}{N_{\rm trig}}\frac{{\rm d}^2N^{\rm pair}}{{\rm d}\Delta\eta{\rm d}\Delta\phi}=B(0,0)\frac{S(\Delta\eta,\Delta\phi)}{B(\Delta\eta,\Delta\phi)}. \tag{6}$$

The normalization factor, $B(0,\,0)$, is the value of the background distribution at $\Delta\eta=0$ and $\Delta\phi=0$.

In order to obtain azimuthal anisotropy harmonics, $v_n\{2\}$, the projection of the two-dimensional correlation function given by Eq. (6) onto the $\Delta\phi$ axis can be Fourier decomposed as given in Eq. (2). In order to suppress the short-range correlations arising from jet fragmentation and resonance decays, an averaging over $|\Delta\eta|>2$ is applied. This is one way to extract the two-particle Fourier coefficients $V_{n\Delta}$ introduced in Eq. (2).

3.2 Principal component analysis

PCA is a statistical method that orders fluctuations in data by size or so-called components. Application of this method in frames of anisotropic flow was introduced in Ref. [24] and further investigated in Refs. [25, 29]. By extracting principal components from the two-particle correlation data one can probe the presence of any event-by-event flow fluctuations.

Section 3.1 shows how the two-particle Fourier harmonics $V_{n\Delta}$ are extracted using the fitting procedure. An alternative approach for calculating the Fourier harmonics $V_{n\Delta}$ is applied in Ref. [18] as,

$$V_{n\Delta}(p_{\rm T}^a,p_{\rm T}^b)=\langle\langle\cos(n\Delta\phi)\rangle\rangle_S-\langle\langle\cos(n\Delta\phi)\rangle\rangle_B, \tag{7}$$

where S and B stand for the signal and for the background, respectively. Here, double brackets $\langle\langle\cdot\rangle\rangle$ denote averaging over charged pion pairs and over all events from the given centrality class. The procedure of forming pairs in S and B, with the pseudo-rapidity cut $|\Delta\eta|>2$, is identical to the fitting case. Following the procedure given in Ref. [24], in order to use the PCA technique a single bracket definition for the two-particle Fourier harmonics $V_{n\Delta}^{\rm PCA}$ is used,

$$V_{n\Delta}^{\rm PCA}(p_{\rm T}^a,p_{\rm T}^b)=\langle\cos(n\Delta\phi)\rangle_S-\langle\cos(n\Delta\phi)\rangle_B, \tag{8}$$

where $\langle\cdot\rangle$ refers to averaging over all events from the given centrality class. The PCA method is applied by doing the eigenvalue decomposition of the covariance matrix that is built out of the $V_{n\Delta}^{\rm PCA}$ harmonics. By defining N_b differential $p_{\rm T}$ bins one can construct the corresponding covariance matrix $[\hat{V}(p_{\rm T}^a,p_{\rm T}^b)]_{N_b\times N_b}$. The diagonal elements are harmonics with correlated particles a and b taken from the same $p_{\rm T}$ bin and the non-diagonal elements are harmonics with correlated particles a and b taken from the different $p_{\rm T}$ bins. In this analysis the $p_{\rm T}$ range, going from 0.3 to 3.0 GeV/c, has been divided into $N_b=7$ non-equidistant $p_{\rm T}$ bins. By solving the eigenvalue problem of the $[\hat{V}(p_{\rm T}^a,p_{\rm T}^b)]_{N_b\times N_b}$ matrix, a set of the eigenvalues, $\lambda^{(\alpha)}$, and eigenvectors, $e^{(\alpha)}$, has been obtained. Here, $\alpha=1,...,N_b$. A new $p_{\rm T}$-dependent observable, $V_n^{(\alpha)}(p_{\rm T})$, is introduced as

$$V_n^{(\alpha)}(p_{\rm T})=\sqrt{\lambda^{(\alpha)}}e^{(\alpha)}(p_{\rm T}), \tag{9}$$

referring to it as mode for the given α. The first mode (denoted with $\alpha=1$) corresponds to the first greatest variance of data, the second mode (denoted with $\alpha=2$) corresponds to the second greatest variance of data and

so on. The modes are not of the same order as the standard $v_n\{2\}$ harmonics and a normalized observable is defined as,

$$v_n^{(\alpha)}(p_{\rm T}) = \frac{V_n^{(\alpha)}(p_{\rm T})}{\langle M(p_{\rm T})\rangle}, \tag{10}$$

where $\langle M(p_{\rm T})\rangle$ denotes the averaged multiplicity in a given $p_{\rm T}$ bin. The multiplicity normalization, introduced in Ref. [24], follows from the fact that the two-particle harmonics from Eq. (7) and Eq. (8) differ by a factor of $\langle N^{\rm pairs}(p_{\rm T},p_{\rm T})\rangle \simeq \langle M(p_{\rm T})\rangle^2$. However, the last equality is broken when the pseudo-rapidity cut $|\Delta\eta|>2$ is applied. Thus, the multiplicity normalization is restored by correcting the PCA harmonics from Eq. (8) as

$$V_{n\Delta}^{\rm PCA}(p_{\rm T}^a,p_{\rm T}^b) \mapsto \frac{N^{\rm pairs}(p_{\rm T}^a,p_{\rm T}^b,|\eta|<2.4)}{N^{\rm pairs}(p_{\rm T}^a,p_{\rm T}^b,|\Delta\eta|>2)} V_{n\Delta}^{\rm PCA}(p_{\rm T}^a,p_{\rm T}^b).$$

The observables from Eq. (10) for $\alpha=1$ and $\alpha=2$ will be referred to as the leading and the sub-leading flow modes respectively. The magnitude of the leading flow mode, $v_n^{(1)}$, should be practically equal to the $v_n\{2\}$ measured using the two-particle correlation method. The CMS Collaboration showed in Refs. [30, 31] that the $p_{\rm T}$ dependence of the leading elliptic and triangular flow modes for pPb collisions at 5.02 TeV and for PbPb collisions at 2.76 TeV data are in excellent agreement with corresponding two-particle measurements presented in Ref. [32] and in Ref. [33], respectively.

4 Results

In order to check the consistency of the extracted azimuthal anisotropies, v_n, using the PCA method and one of the standard approaches like Fourier decomposition given by Eq. (2), as well as to perform a PCA analysis to extract the leading and sub-leading flow modes, the two-particle correlation functions defined by Eq. (6) are constructed. For each centrality interval, ranging from the ultra-central 0–0.2% to the peripheral 50%–60%, two-particle correlation functions for 7 $p_{\rm T}$ intervals between 0.3 and 3.0 GeV/c are formed. Thus, 7 diagonal and 21 non-diagonal two-particle correlation functions are produced. As examples, in Fig. 1 are shown two-dimensional, in $\Delta\eta$ and $\Delta\phi$, two-particle correlation functions from HYDJET++ PbPb simulations at $\sqrt{s_{\rm NN}}$=2.76 TeV where both particles are in the range $0.3<p_{\rm T}<0.5$ GeV/c (left-hand column) and $1.5<p_{\rm T}<2.0$ GeV/c (middle column) (diagonal elements), while in the right-hand column one particle is in the range $0.3<p_{\rm T}<0.5$ GeV/c and the other in $1.5<p_{\rm T}<2.0$ GeV/c (non-diagonal element).

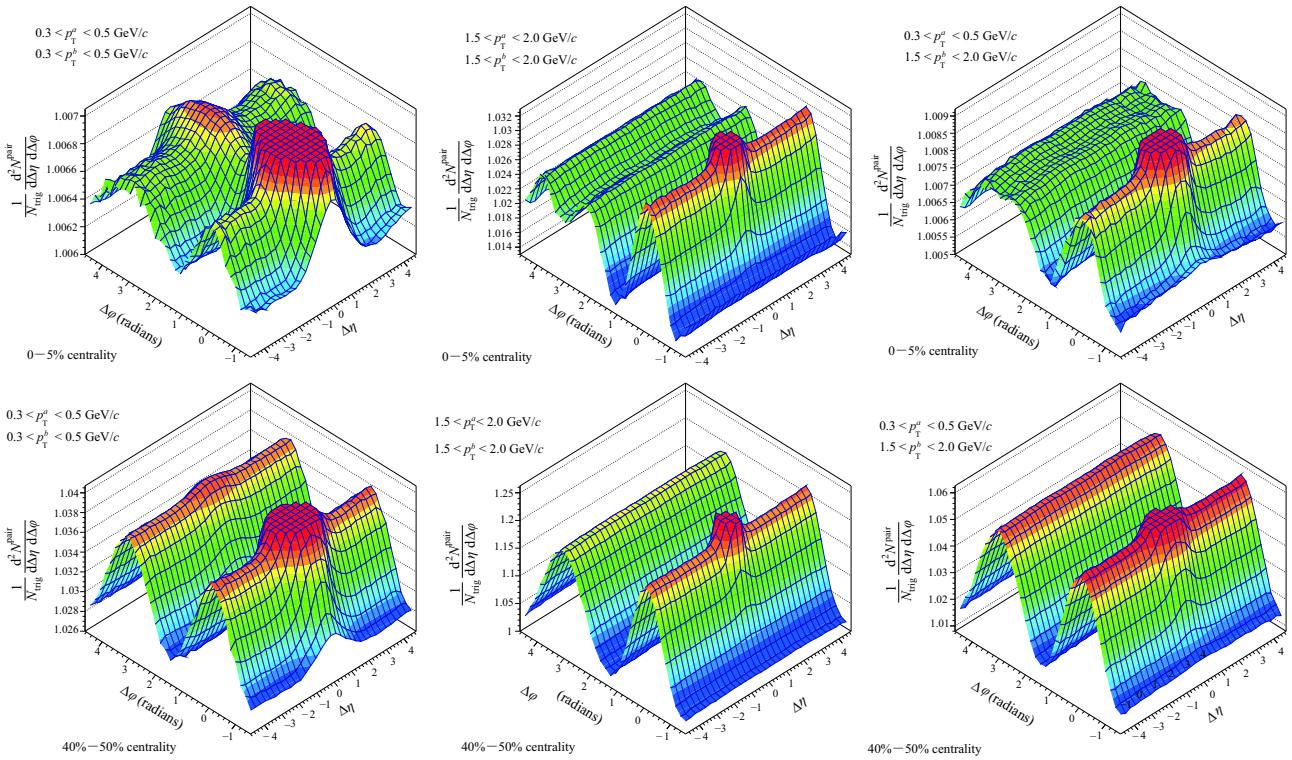

Fig. 1. Two dimensional, in $\Delta\eta$ and $\Delta\phi$, two-particle correlation functions where both particles are in the range $0.3<p_{\rm T}<0.5$ GeV/c (left column), $1.5<p_{\rm T}<2.0$ GeV/c (middle column) and where one particle is in the range $0.3<p_{\rm T}<0.5$ GeV/c and the other in $1.5<p_{\rm T}<2.0$ GeV/c (right column). Top (bottom) row: The correlation functions are constructed from very central 0-5% (peripheral 40%–50%) 2.76 TeV PbPb collisions simulated with the HYDJET++ model using the 'flow + quenched jets' switch.

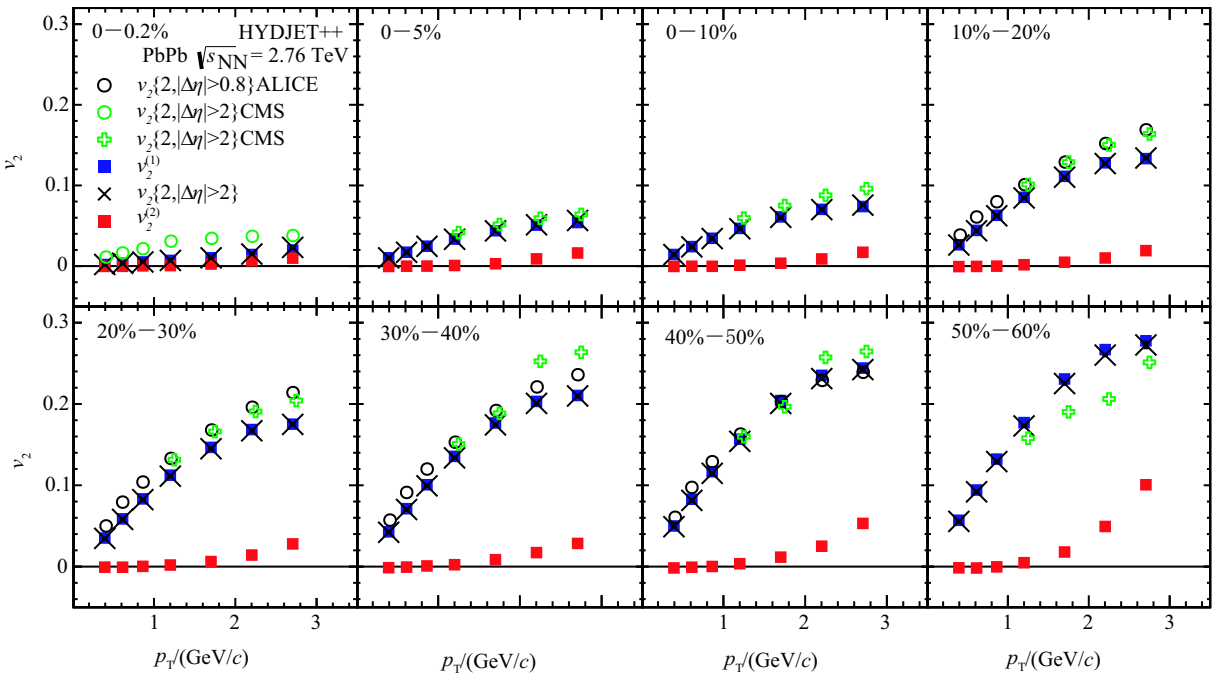

Fig. 2. The leading ($\alpha = 1$) and sub-leading ($\alpha = 2$) flow mode for the $n = 2$ harmonic as a function of p_T measured using the PCA approach in a wide centrality range of PbPb collisions at 2.76 TeV generated with the HYDJET++ model. The $v_2^{(1)}$ results are compared to the $v_2\{2\}$ measured by the CMS Collaboration in Ref. [18] (open green circles) and Ref. [15] (open green crosses) and by the ALICE [33] Collaboration, and to the $v_2\{2,|\Delta\eta|>2\}$ extracted from the same HYDJET++ simulation using the two-particle correlation method. The error bars correspond to statistical uncertainties.

The correlation functions in the top row are constructed from very central 0–5% collisions, and those from peripheral 40%–50% collisions are presented in the bottom row. As this analysis deals with the long-range correlations, the near side peak is truncated. One can see that, beside the short-range correlated near side peak, the HYDJET++ model can reproduce rather well features of the elliptic and triangular flow. For higher transverse momenta ($1.5 < p_T < 2.0$ GeV/c), in the difference of peripheral collisions where the elliptic flow dominates, in central collisions (0–5% centrality) the magnitude of the v_3 becomes similar to the magnitude of the v_2, and thus a clear double-bump peak is seen at the away side.

In Fig. 2 are shown the PCA results for the leading and sub-leading flow modes for the second harmonic in 8 centrality regions ranging from ultra-central (0–0.2%) to peripheral (50%–60%) PbPb collisions at $\sqrt{s_{NN}} = 2.76$ TeV simulated with the HYDJET++ event generator. The leading flow mode, $v_2^{(1)}$, is dominant and describes the experimentally measured $v_2\{2\}$ from two-particle correlations taken from Ref. [18] and Ref. [33] rather well. Additionally, due to consistency, in Fig. 2 are also shown $v_2\{2,|\Delta\eta| > 2\}$ values measured using two-particle correlations constructed from the same HYDJET++ generated data. In Fig. 2 these results are depicted with crosses and show an excellent agreement with $v_2^{(1)}$ extracted using the PCA method. The extracted $v_2^{(1)}$ has the expected centrality behavior: a small magnitude at ultra-central collisions which then gradually increases going to peripheral collisions. The newly observed sub-leading flow mode of second order harmonic, $v_2^{(2)}$, is practicaly equal to zero at small-p_T for all centrality bins. For $p_T > 2$ GeV/c, the sub-leading flow mode has a small positive value and slowly increases going from semi-central to peripheral PbPb collisions. The CMS Collaboration presented the experimentally measured leading and sub-leading flow mode in PbPb collisions within the same p_T range and for the same centrality bins in Refs. [30, 31]. Besides the leading flow mode, the HYDJET++ predictions for the sub-leading flow mode are also in qualitative agreement with the experimental findings from Refs. [30, 31]. For centralities above 30%, the $v_2^{(2)}$ magnitudes predicted by the HYDJET++ model are slightly larger than those observed from the experimental data.

Similarly to in Fig. 2, in Fig. 3 are shown the PCA leading and sub-leading flow mode predictions of the HYDJET++ model for the third harmonic. Again, the results are extracted from the 8 centrality regions, the same as in Fig. 2, of PbPb collisions at $\sqrt{s_{NN}}$= 2.76 TeV. The $v_3^{(1)}$ is in rather good agreement with the $v_3\{2\}$ results

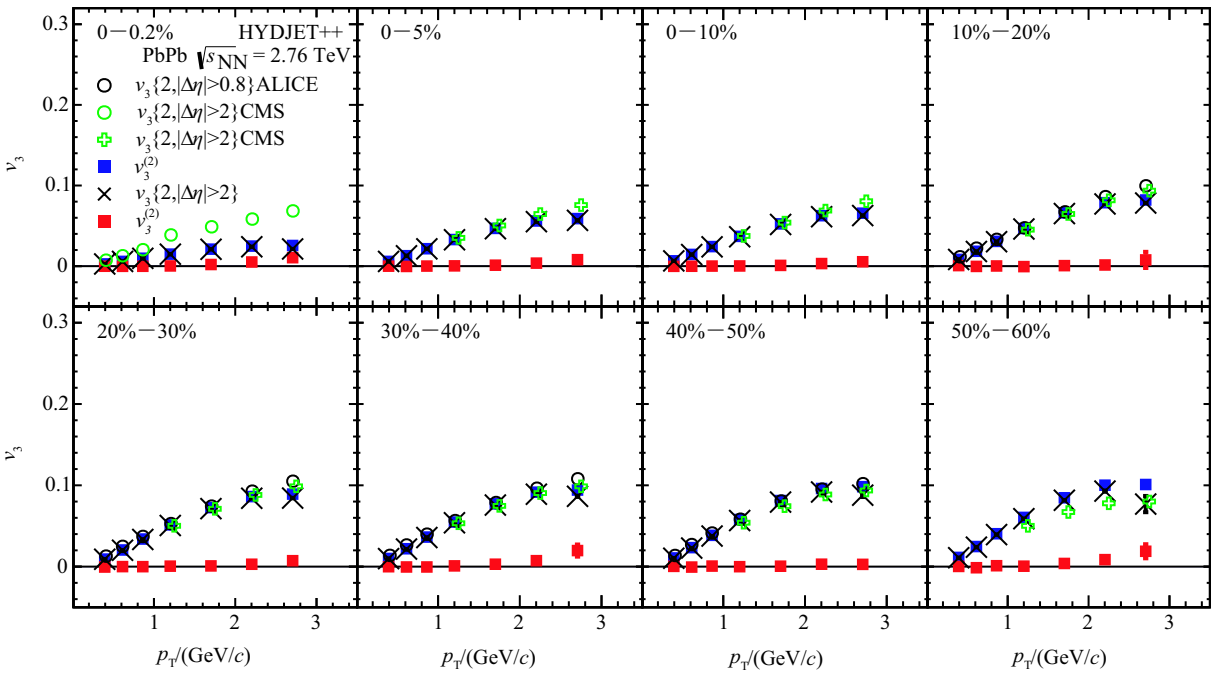

Fig. 3. The leading ($\alpha = 1$) and sub-leading ($\alpha = 2$) flow mode for the $n = 3$ harmonic as a function of p_T measured using the PCA approach in a wide centrality range of PbPb collisions at 2.76 TeV generated with the HYDJET++ model. The $v_3^{(1)}$ results are compared to the $v_3\{2\}$ measured by the CMS Collaboration in Ref. [18] (open green circles) and Ref. [15] (open green crosses) and by the ALICE [33] Collaboration, and to the $v_3\{2,|\Delta\eta|>2\}$ extracted from the same HYDJET++ simulation using the two-particle correlation method. The error bars correspond to statistical uncertainties.

measured using two-particle correlations taken from Ref. [18] and Ref. [33], except in the case of ultra-central collisions. Also, the $v_3\{2\}$ extracted from the two-particle correlations formed from the same HYDJET++ generated data are in an excellent agreement with the $v_3^{(1)}$ obtained from the PCA method. The sub-leading mode is, up to 3 GeV/c, almost equal to zero. This supports the finding from Refs. [19, 23] that the third harmonic factorizes better than the second one. Also, the small $v_3^{(2)}$ values extracted from HYDJET++ simulated PbPb events are in an agreement with those found in Refs. [30, 31] extracted from the experimental PbPb data.

To summarize the results, in Fig. 4 are depicted the ratios[1)] between the sub-leading and leading flow mode. The ratio is calculated from the values taken from $2.5 < p_T < 3.0$ GeV/c, where the effect is strongest. The results are presented as a function of centrality. The results in the top panel of Fig. 4 show that in the case of $n = 2$ the strength of the relative magnitude $v_2^{(2)}/v_2^{(1)}$ is smallest for events with centralities between 10% and 30%, i.e. where the elliptic flow is most pronounced. Going to very central collisions, the magnitude of the effect dramatically increases. Also, the effect reaches a significant magnitude going to peripheral collisions. Qualitatively, such behavior is in agreement with the r_2 multiplicity dependence presented in Ref. [19]. Centrality

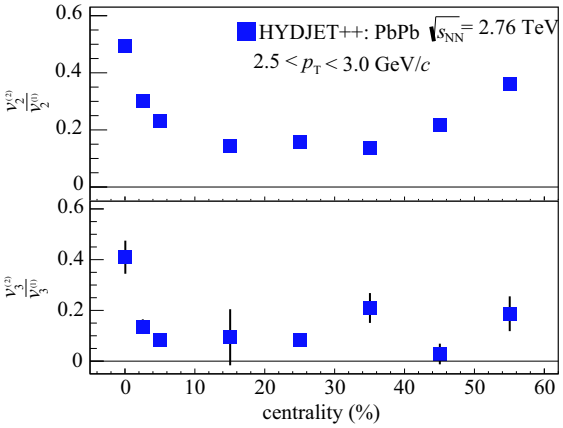

Fig. 4. The ratio between values of the sub-leading and leading flow, taken for the highest p_T bin, as a function of centrality calculated using the PCA method applied to PbPb collisions at $\sqrt{s_{NN}} = 2.76$ TeV simulated with the HYDJET++ event generator. The error bars correspond to statistical uncertainties.

1) According to Eq. (2) in Ref. [25], the connection to the factorization breaking variable is given through ratio $v_n^{(2)}/v_n^{(1)}$ which gives the relative strength of the effect.

of the dependence ratio which corresponds to the $n=3$ case is shown in the bottom panel of Fig. 4. The $v_3^{(2)}/v_3^{(1)}$ ratio, integrated over all centralities, is 0.095 ± 0.009. As the extracted $v_3^{(2)}$ values are small, small fluctuations in their values can easily produce a non-smooth distribution, shown in the bottom panel of Fig. 4. The overall small $v_3^{(2)}$ values found in this analysis are also in qualitative agreement with the r_3 multiplicity dependence presented in Ref. [19].

5 Discussion

To explore the origin of the sub-leading flow signal observed within the HYDJET++ model, besides the analysis of the PbPb data obtained using the 'flow + quenched jets' switch, for which the results were shown in Section 4, the pure 'flow' switch has also been used to generate PbPb collisions at $\sqrt{s_{\rm NN}}=2.76$ TeV. The comparisons between the PCA elliptic and triangular flow results obtained using these two switches are shown in Fig. 5 and Fig. 6, respectively. As expected, the pure 'flow' HYDJET++ switch gives a linearly increasing leading flow mode for both $v_n^{(1)}$ harmonics $n=2$ and 3. Also, as expected, the corresponding magnitude, at a given $p_{\rm T}$, is greater with respect to that extracted from the data obtained using the 'flow + quenched jets' switch. The results for the sub-leading flow mode obtained using the pure 'flow' switch, contrary to those shown in Section 4, are consistent with zero for centralities smaller than 20%. But, even in the case of the pure 'flow' switch, for centralities above 20% a modest effect of the sub-leading flow starts to appear. Up to the centrality of 40% the magnitude of the effect is still smaller than both the experimental findings from Refs. [30, 31] and from the results obtained using the 'flow + quenched jets' switch. For the most peripheral, 50%–60%, the $v_2^{(2)}$ magnitude at high enough $p_{\rm T}$ is greater than both the experimental result and that obtained with the 'flow + quenched jets' switch.

At first glance, it seems that the HYDJET++ data simulated using the pure 'flow' switch should not show the existence of the sub-leading flow modes. But, resonance decays and fluctuations of particle momenta together with the topology of peripheral events [34] could imitate hot-spots which at the end could produce non-zero sub-leading flows. The HYDJET++ data simulated with 'flow + quenched jets' could have charged pions coming from the jet fragmentation, due to the interaction with the soft medium and because the different path length with respect to the flow symmetry plane can increase the abundance of such high-$p_{\rm T}$ pions near the flow symmetry plane. This could also produce the above-mentioned hot-spots and consequently sub-leading flows.

The results for the sub-leading triangular flow mode are presented in Fig. 6. Similar to the 'flow + quenched jets' results shown in Section 4, the $v_3^{(2)}$ values, calculated using the pure 'flow' switch, are close to zero for all centralities and at all $p_{\rm T}$. This again shows that the

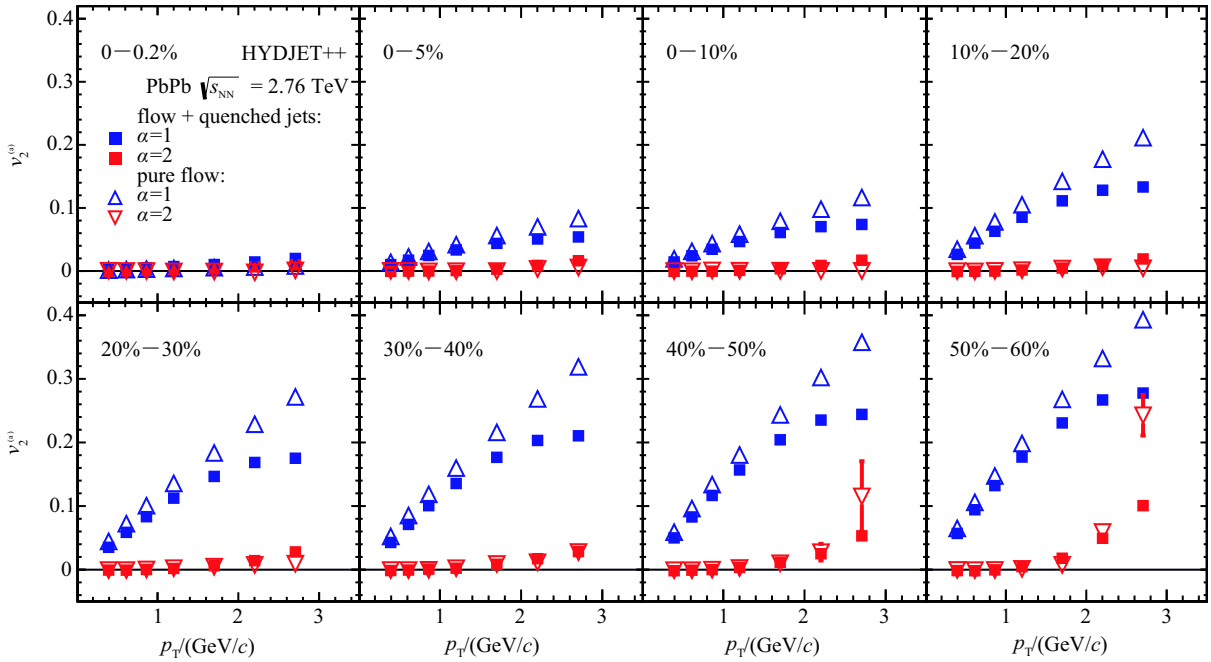

Fig. 5. The leading ($\alpha=1$) and sub-leading ($\alpha=2$) flow mode for the $n=2$ harmonic as a function of $p_{\rm T}$ measured using the PCA approach in a wide centrality range of PbPb collisions at 2.76 TeV generated with the HYDJET++ model with the pure 'flow' switch (triangles) and with the 'flow + quenched jets' switch (squares). The error bars correspond to statistical uncertainties.

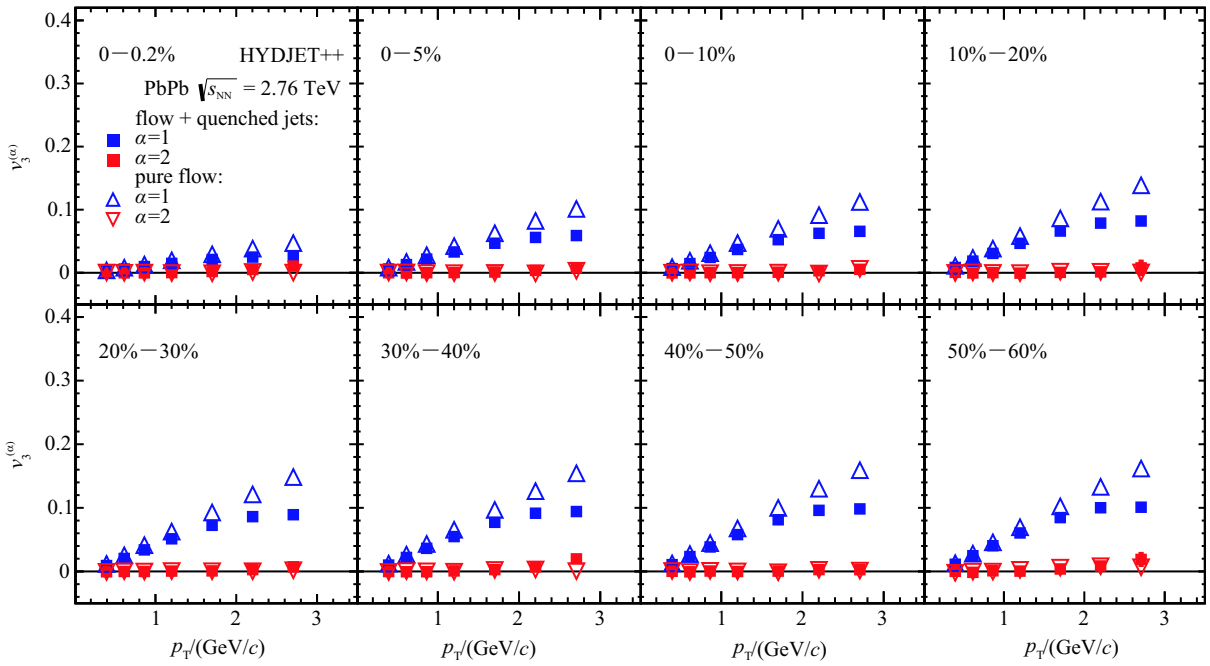

Fig. 6. The leading ($\alpha = 1$) and sub-leading ($\alpha = 2$) flow mode for the $n = 3$ harmonic as a function of p_T measured using the PCA approach in a wide centrality range of PbPb collisions at 2.76 TeV generated with the HYDJET++ model with the pure 'flow' switch (triangles) and with the 'flow + quenched jets' switch (squares). The error bars correspond to statistical uncertainties.

assumption of the factorization of the two-particle Fourier coefficients into a product of the v_3 anisotropy harmonics in the case of the pure 'flow' switch is fully valid.

The Pearson coefficient, used to measure the magnitude of factorization breaking, is defined [19, 24] as

$$r_n(p_T^a,p_T^b) = \frac{V_{n\Delta}(p_T^a,p_T^b)}{\sqrt{V_{n\Delta}(p_T^a,p_T^a)V_{n\Delta}(p_T^b,p_T^b)}} \sim\langle\cos n(\Psi_n(p_T^a)-\Psi_n(p_T^b))\rangle. \quad (11)$$

The r_n ratio, which is proportional to the cosine term, is equal to one if the flow symmetry plane angle is a global quantity. If the factorization breaking occurs then the value of r_n becomes smaller than one. In Ref. [24] it is shown that the principal component analysis approximates the two-particle Fourier coefficient as

$$V_{n\Delta}(p_T^a,p_T^b)=\sum_{\alpha=1}^{N_b} V_n^{(\alpha)}(p_T^a)V_n^{(\alpha)*}(p_T^b), \quad (12)$$

where each term in the sum corresponds to a different mode α of the flow fluctuations introduced with Eq. (9). Factorization breaking occurs when non-zero terms with $\alpha \geqslant 2$ appear in the above sum. Equation (12) is used to reconstruct the $V_{n\Delta}$ coefficients from the $V_n^{(\alpha)}$ flow modes extracted using principal component analysis. In order to connect the results for the sub-leading flow modes

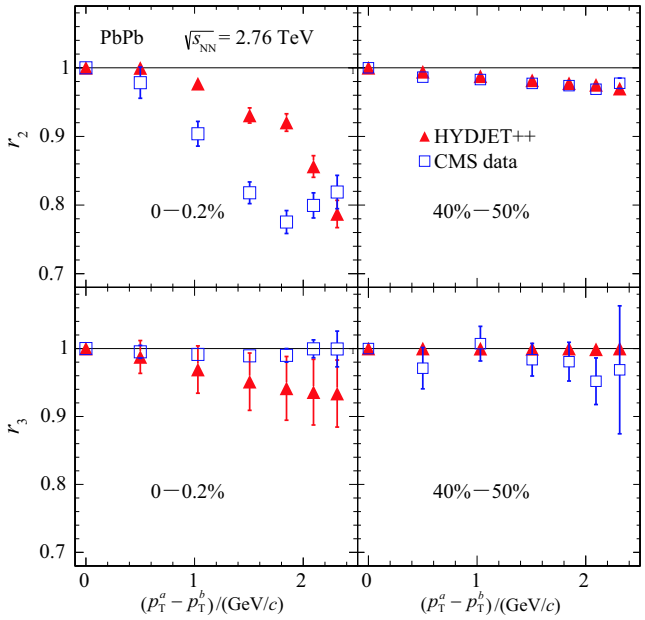

Fig. 7. Comparison of r_2 (top row) and r_3 (bottom row) reconstructed with harmonic decomposition using the leading and sub-leading flow mode extracted from the HYDJET++ model with the experimental r_2 and r_3 values taken from Ref. [19] for the ultra-central 0–0.2% and peripheral 40%–50% centrality classes in PbPb collisions at $\sqrt{s_{NN}}$ = 2.76 TeV. The error bars correspond to statistical uncertainties.

extracted from HYDJET++ generated PbPb collisions at 2.76 TeV with the experimentally seen initial-state fluctuations [19], in Fig. 7 is shown a comparison between the r_2 and r_3 ratios, depicted as a function of the transverse momentum difference $p_{\rm T}^a$–$p_{\rm T}^b$, measured experimentally in Ref. [19] and extracted from the HYDJET++ model and calculated using Eq. (11) and Eq. (12). The comparison is performed only in the ultra-central (0–0.2% centrality) and peripheral (40%–50% centrality) collisions, i.e. where the factorization effect is largest. Using in Eq. (12) only the leading and sub-leading flow mode ($N_b = 2$) one observes a fair reconstruction of r_n ratios[1)]. To improve the reconstruction of r_2 in ultra-central collisions, where the effect of the initial-state fluctuations dominates, one would need to add additional modes ($\alpha \geqslant 3$) in the two-particle harmonic decomposition. As in the case of the elliptic flow, the sub-leading flow mode corresponding to the triangular flow captures the small factorization effect well.

6 Conclusions

The PCA method for studying flow, by its construction, may fully exploit the information contained in the covariance matrix formed from the two-particle Fourier coefficients and thus may provide high sensitivity not only to the standard defined flow measurements, but also to the influence of the initial-state fluctuations on the hydrodynamic flow. In the difference of two-particle correlation method, where the information was calculated by integrating over the momentum of one of particles which form the pair, within the PCA approach, the detailed information depends on the momenta of both particles of the pair. As the leading flow mode represents the hydrodynamic response to the average geometry, it is essentially equal to the anisotropy harmonics measured using the two-particle correlations method. The sub-leading mode can be understood as the response to the event-by-event initial-state fluctuations which are the main source of the factorization-breaking effect.

The PCA analysis of the PbPb collisions simulated by the HYDJET++ model at $\sqrt{s_{\rm NN}} = 2.76$ GeV shows that the leading flow mode, $v_n^{(1)}$, for n=2,3 represents the dominant mode and qualitatively describes the experimentally measured v_n from two-particle correlations. Additionally, the HYDJET++ model also shows the existence of the sub-leading flow mode $v_n^{(2)}$, with a magnitude in rather good agreement with the experimental results from the CMS Collaboration. Also, the r_2 and r_3 ratios calculated from only leading and sub-leading flow modes extracted from the HYDJET++ model data using PCA fairly reconstructs experimentally measured ratios. This analysis may also provide new insights into the possible influence of the dynamics of the collision on the appearance of the sub-leading flow modes, and help to understand and improve modeling of the evolution of strongly-coupled quark gluon plasma.

The authors would like to thank Igor Lokhtin and his group from Skobeltsyn INP MSU for providing us with HYDJET++ code and for useful sugestions.

References

1 J. -Y. Ollitrault, Phys. Rev. D, **48**: 1132–1139 (1993)
2 S. Voloshin and Y. Zhang, Z. Phys. C, **70**: 665–672 (1996)
3 A. M. Poskanzer and S. A. Voloshin, Phys. Rev. C, **58**: 1671–1678 (1998)
4 B. Alver and G. Roland, Phys. Rev. C, **81**: 054905–054913 (2010)
5 B.B. Back et al (PHOBOS Collaboration), Phys. Rev. Lett., **89**: 222301 (2002)
6 K.H. Adams et al (STAR Collaboration), Phys. Rev. Lett., **86**: 402–407 (2001)
7 K. Adcox et al (PHENIX Collaboration), Phys. Rev. Lett., **89**: 212301 (2002)
8 K. Aamodt et al (ALICE Collaboration), Phys. Rev. Lett., **105**: 252302 (2010)
9 K. Aamodt et al (ALICE Collaboration), Phys. Rev. Lett., **107**: 032301 (2011)
10 B.B. Abelev et al (ALICE Collaboration), JHEP, **1506**: 190–271 (2015)
11 J. Adam et al (ALICE Collaboration), Phys. Rev. Lett., **116**: 132302 (2016)
12 G. Aad et al (ATLAS Collaboration), Phys. Lett. B, **707**: 330–348 (2012)
13 G. Aad et al (ATLAS Collaboration), Phys. Rev. C, **86**: 014907–014954 (2012)
14 G. Aad et al (ATLAS Collaboration), JHEP, **11**: 183–240 (2013)
15 S. Chatrchyan et al (CMS Collaboration), Eur. Phys. J. C, **72**: 2012 (2012)
16 S. Chatrchyan et al (CMS Collaboration), Phys. Rev. C, **87**: 014902–014936 (2013)
17 S. Chatrchyan et al (CMS Collaboration), Phys. Rev. C, **89**: 044906–044937 (2014)
18 S. Chatrchyan et al (CMS Collaboration), JHEP, **02**: 088–0126 (2014)
19 V. Khachatryan et al (CMS Collaboration), Phys. Rev. C, **92**: 034911–034937 (2015)
20 S. Wang et al, Phys. Rev. C, **44**: 1091–1095 (1991)
21 F. G. Gardim, F. Grassi, M. Luzum, and J.-Y. Ollitrault, Phys. Rev. C, **87**: 031901–031906 (2013)
22 U. Heinz, Z. Qiu, and C. Shen, Phys. Rev. C, **87**: 034913–034922 (2013)
23 Y. Zhou, Nucl. Phys. A, **931**: 949–953 (2014)
24 R. Bhalerao, J.-I. Ollitrault, S. Pal, and D. Teaney, Phys. Rev. Lett., **114**: 152301–152306 (2015)
25 A. Mazeliauskas and D. Teaney, Phys. Rev. C, **91**: 044902–044912 (2015)

1) The difference in the size of the statistical uncertainties comes because of different statistics used in the experiment and in the HYDJET++ model.

26 I. P. Lokhtin, L.V. Malinina, S. V. Petrushanko, A. M. Snigirev, I. Arsene, and K. Tywoniuk, Comput. Phys. Commun., **180**: 779–799 (2009)
27 T. Sjostrand, S. Mrenna, and P. Skands, JHEP, **0605**: 026–0602 (2006)
28 I. P. Lokhtin and A. M. Snigirev, Eur. Phys. J. C, **45**: 211–217 (2006)
29 A. Mazeliauskas and D. Teaney, Phys. Rev. C, **93**: 024913–024928 (2016)
30 CMS Collaboration, Principal Component Analysis of Two-Particle Azimuthal Correlations in PbPb and pPb Collisions at CMS (CERN Document Server, 2015), http://cds.cern.ch/record/2055291. Accessed 27 September 2015
31 J. Milosevic et al (CMS Collaboration), Nucl. Phys. A, **956**: 308–311 (2016)
32 S. Chatrchyan et al (CMS Collaboration), Phys. Lett. B, **724**: 213–240 (2013)
33 K. Aamodt et al (ALICE Collaboration), Phys. Lett. B, **708**: 249–264 (2012)
34 L. V. Bravina, E. S. Fotina, V. L. Korotkikh, I. P. Lokhtin, L. V. Malinina,E. N. Nazarova, S. V. Petrushanko, A. M. Snigirev, and E. E. Zabrodin, Eur. Phys. J. C, **75**, 588–598 (2015)